Progress In Electromagnetics Research Letters, Vol. 104, 121–129, 2022

Design of a Wideband Antenna for 5G Indoor Base Station Application

Shihao Wu[1, *] and Haoran Shi[2]

Abstract—This paper presents a broadband antenna for 5G indoor micro base station, which has a low profile and simple structure. The proposed antenna avoids the traditional high-cost multilayer technology and is a low-cost configuration. It consists of a center fed circular patch with four shorting pins to properly stimulate the radiation mode of TM_{01} and TM_{31} internally. Next, four equally sized fan-shaped slots are opened in the radiator to further expand the bandwidth and improve the input impedance. $|S_{11}| < -10$ dB simulation impedance bandwidth is about 51% from 3.11 to 5.24 GHz and covers 5Gn78 (3.3–3.8 GHz), n77(3.3–4.2 GHz) and n79 (4.4–5 GHz). The voltage standing wave ratio (VSWR) < 1.8 in the whole operating frequency band, which has good matching characteristics.

1. INTRODUCTION

The Third Generation Partnership Program (3GPP) divides the sub-6 GHz band into N77 (3.3–4.2 GHz), N78 (3.3–3.8 GHz), and N79 (4.4–5 GHz) for 5G applications in different countries. As 5G is characterized by high frequency and fast attenuation, it is difficult to cover indoor signals only by relying on outdoor base stations. It is a challenge to design an indoor base station antenna that contains the above frequencies to provide a degree of power compensation. The omnidirectional broadband antenna with conical radiation pattern can provide 360° coverage of indoor signals and are the most common choice [1].

The traditional monopole antenna is a typical vertically polarized antenna with an omnidirectional radiation pattern, but it has a high profile (1/4 wavelength) and a narrow bandwidth (8%–16%) [2]. As a result, the researchers proposed a number of improvements to previous designs of monopole antennas. A broadband monopole antenna was proposed, which effectively expanded the low-frequency bandwidth by loading coupling elements [3]. However, the profile of the antenna was high. In [4], Delaveaud et al. proposed a monopole antenna with a short wire structure. The antenna is small in size and has a low profile, but the bandwidth of the antenna is only 3%. The antenna bandwidth in [5] and [6] is significantly improved, but it has the disadvantage of low gain (< 4 dBi).

Microstrip patch antennas have the advantages of low profile and are easy to integrate, so they are suitable for the use in small systems. In [7], a microstrip antenna applied to indoor communication system was proposed, with a profile height of $0.052\lambda_0$ but a bandwidth of only 7.1%. Considering the impact of feed structure on bandwidth, an L-shaped probe feed structure was proposed in [8] and [9], which achieved bandwidths of 27% and 30%, respectively, but this method increases the profile height. Subsequently, a conical radiation pattern was generated by using a concentric ring structure to excite high order modes TM_{21} and TM_{41}, but the feeding was complicated [10]. The circular patch antenna fed by the center can generate a monopole radiation mode [11] and can be theoretically analyzed by the cavity model to meet the requirements of low profile, but the bandwidth of this type of antenna

Received 28 March 2022, Accepted 25 May 2022, Scheduled 11 June 2022

* Corresponding author: Shihao Wu (2632116266@qq.com).

[1] School of Science, Xi'an University of Posts and Telecommunications, Xi'an, Shaanxi 71012, China. [2] School of Electronic Engineering, Xi'an University of Posts and Telecommunications, Xi'an, Shaanxi 71012, China.

is still very narrow [12]. To solve this problem, some researchers increased the bandwidth by loading shorting structures [13]. In [13], 18% bandwidth was achieved through excitation and combination of TM_{01} mode and TM_{02} mode. In addition, the way of increasing ring coupling can also expand the bandwidth. Liu et al. achieved 27.4% higher bandwidth by using double ring coupling [14].

In this paper, we design a micro base station antenna for a 5G indoor system using a circular patch structure loaded with shorting pins. The cavity model method is used to explain the principle and give the design idea. The proposed antenna can provide 51% bandwidth with a profile of $0.05\lambda_{\min}$ and can fully cover 5G-N77, N78 and N79 bands.

2. ANTENNA DESIGN

2.1. Antenna Configuration

The specific structure of the antenna is shown in Fig. 1. It consists of a printed round patch, four rotated fan-shaped grooves, earthed shorting pins, a coaxial probe, and a round metal ground. The circular patch is printed on the surface of an FR4 dielectric plate. The relative dielectric constant is 4.4, and the thickness is 0.5 mm.

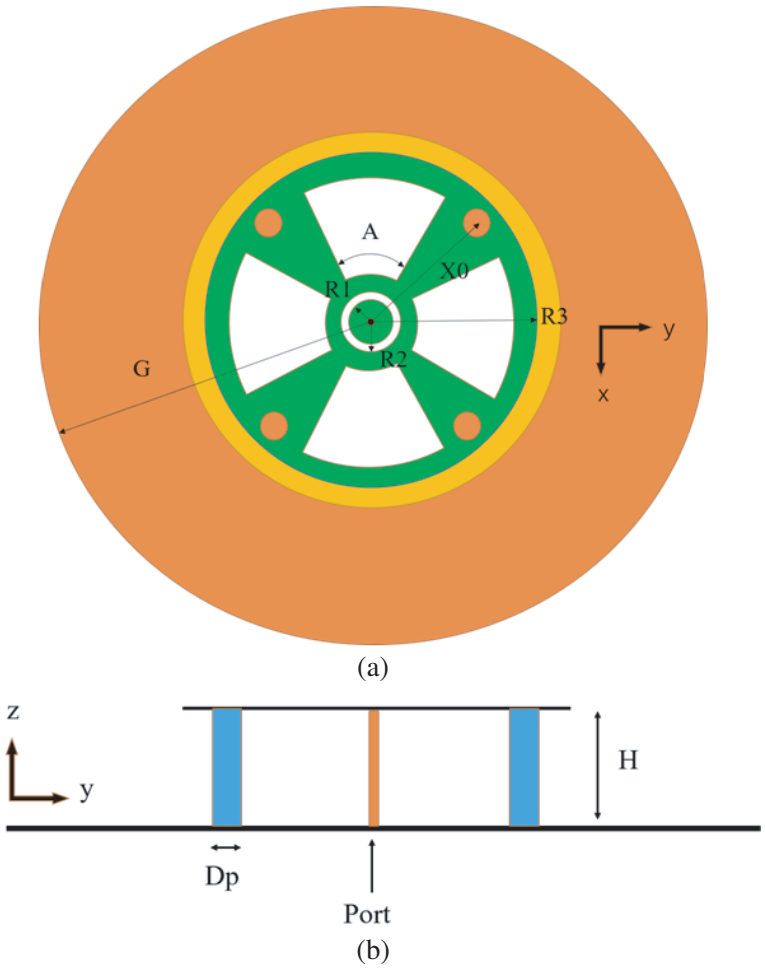

Figure 1. Configuration of the Proposed antenna. $R1 = 1.9\,\text{mm}$, $R2 = 3\,\text{mm}$, $R3 = 20\,\text{mm}$, $X0 = 13\,\text{mm}$, $A = 28\,\text{deg}$, $H = 5\,\text{mm}$, $G = 46\,\text{mm}$, $Dp = 2.4\,\text{mm}$. (a) Top view. (b) Side view.

2.2. Antenna Design

Considering that the resonant frequency of the low-order mode is easier to adjust, it can be matched with the higher-order mode by tuning the resonant frequency of the low-order mode upward, so the radius of the patch is designed based on the higher-order mode.

The size of the circular patch antenna can be calculated by the following formula:

$$f_{nm} = \frac{\chi_{nm} \cdot c}{2\pi a_{eff}\sqrt{\varepsilon_r}} \tag{1}$$

where c represents the speed of light in free space, and χ_{nm} is the mth root of the derivative of the n-order Bessel function. For TM_{31} mode, it corresponds to $\chi_{31} = 4.201$.

The equivalent radius a of the circular patch can be calculated by the following formula [2]:

$$a_{eff} = a\left\{1 + \frac{2h}{\pi a\varepsilon_r}\left(\ln\frac{\pi a}{2h} + 1.7726\right)\right\}^{\frac{1}{2}} \tag{2}$$

Circular cavity mode theory assumes that the magnetic field component at the edge of the patch is negligible. In fact, fringing effect will occur at the edge of the patch. The strength of fringing effect is related to the size of the patch, the thickness of the medium, and the relative dielectric constant. If the edge field of the resonator is ignored, there will be a deviation between the theoretical and actual resonance frequencies [15]. Although the fringing effect becomes smaller ($a/h \gg 1$), it should not be ignored. At this point, a_{eff} can be used as a design guide to determine the radius of the circular patch.

In addition, it can be known from the above formula that the resonant frequency of the antenna is related to the relative dielectric constant ε_r. Due to $\chi_{01} = 0$, there is no resonant frequency in TM_{01} mode in the original pure circular patch antenna. However, ε_r can be changed by introducing the structure of shorting pins and gaps, so as to excite TM_{01} mode and realize the monopole radiation characteristics.

Figure 2 shows the electric field distribution of the proposed antenna in the two resonant modes, respectively. As shown in Fig. 2(a), the electric field on the patch always radiates in a consistent upward direction. This is the radiation property of the monopole, which resonates at low frequencies of 3.3 GHz. The electric field in Fig. 2(b) radiates along both sides of the patch, which is a wide-sided radiation mode and generates a second resonance at 4.8 GHz. The simultaneous excitation of these two modes results in a conical radiation pattern, which is omnidirectional along the horizontal plane. Furthermore, by adjusting the annular groove between the circular patch and annular patch to control the distance between the two radiation modes, the purpose of expanding the bandwidth can be achieved, and the input impedance can be improved to a certain extent.

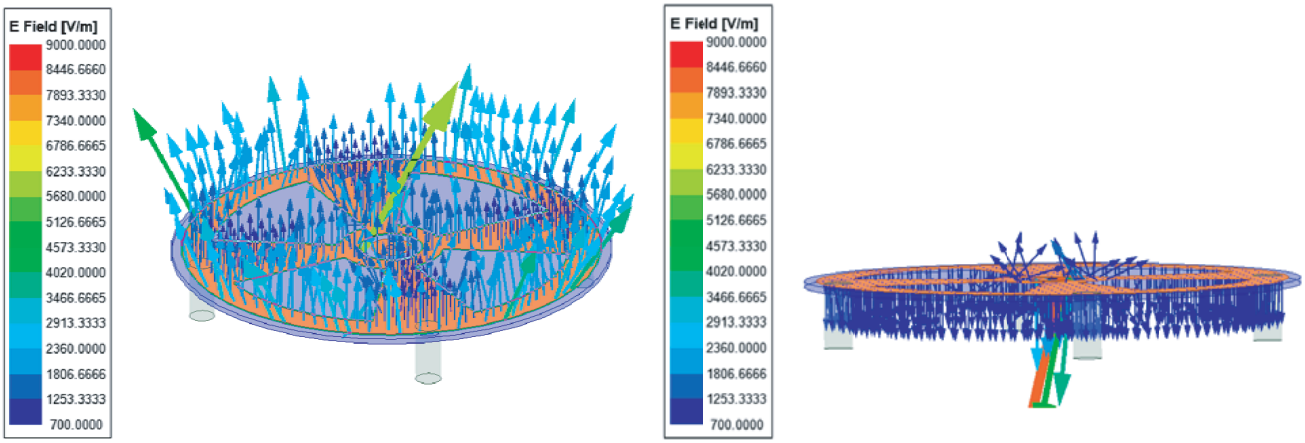

(a) (b)

Figure 2. Electric field distribution of a short-circuited ring patch. (a) 3.3 GHz. (b) 4.8 GHz.

2.3. Parameter Study

In this part, some important parameters which affect the performance of antenna are studied and analyzed.

Figure 3 shows the effect of pin position changes on antenna performance. It can be seen that the location of the pin will have a great influence on the resonance frequency in TM_{01} mode. When pin parameters are properly selected, the two modes are combined into one operating band.

Figure 4 shows the influence of different sizes of the central circular patch. The width of the annular groove can be controlled by adjusting the size of the central circular patch. On the one hand, it will affect the capacitance reactance to some extent, which can be used to balance the inductance

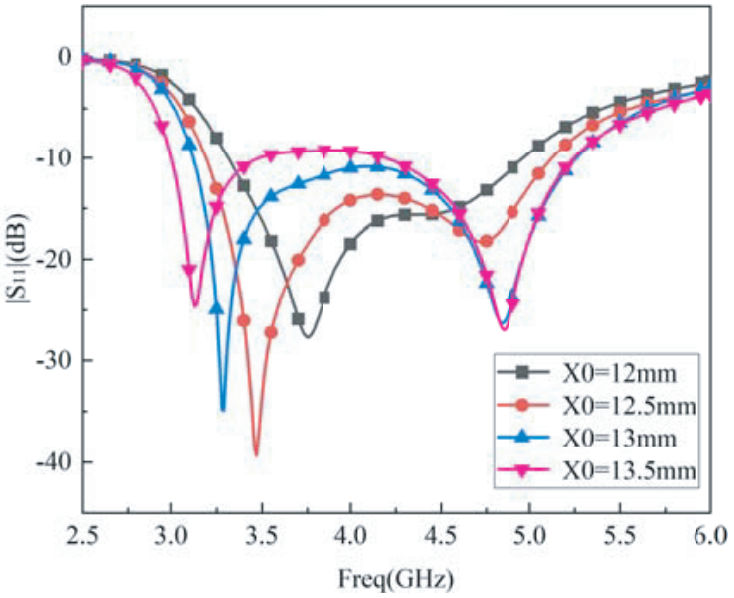

Figure 3. The influence of pin position $X0$ on return loss.

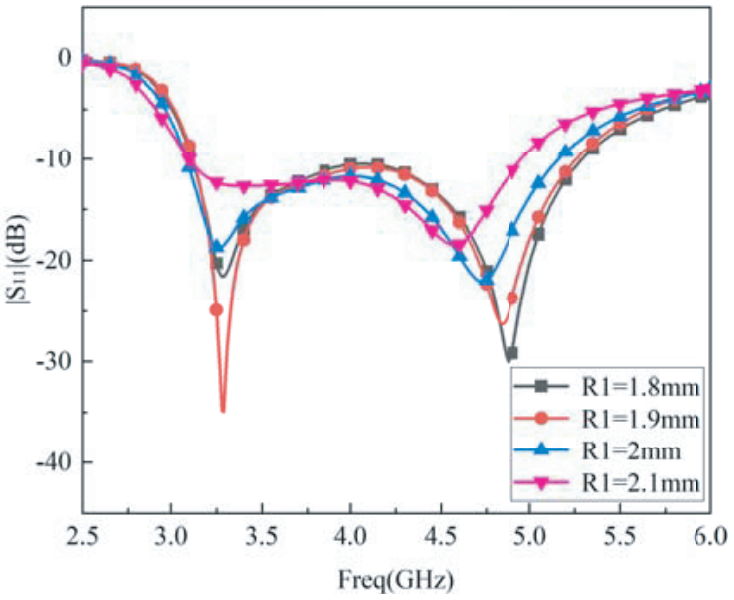

Figure 4. Influence of radius $R1$ of central circular patch on return loss.

characteristics caused by the feed, so as to improve the impedance matching. On the other hand, as the annular groove gradually decreases, it also means that the coupling strength increases, so that the resonant frequency moves to the low frequency. Meanwhile, due to the influence of the coupling effect, the quality factor Q of the antenna will decrease, thus widening the bandwidth. Therefore, at different groove widths, the proposed antenna will present different bandwidths.

Figure 5 compares the effects of cutting four fan-shaped slots on antennas. It can be observed that the frequency changes little at low frequencies, while the high-frequency resonance moves towards lower frequencies. At the same time, the change of reactance brought by the slot will affect the surface current on the patch, which will further affect the antenna input impedance.

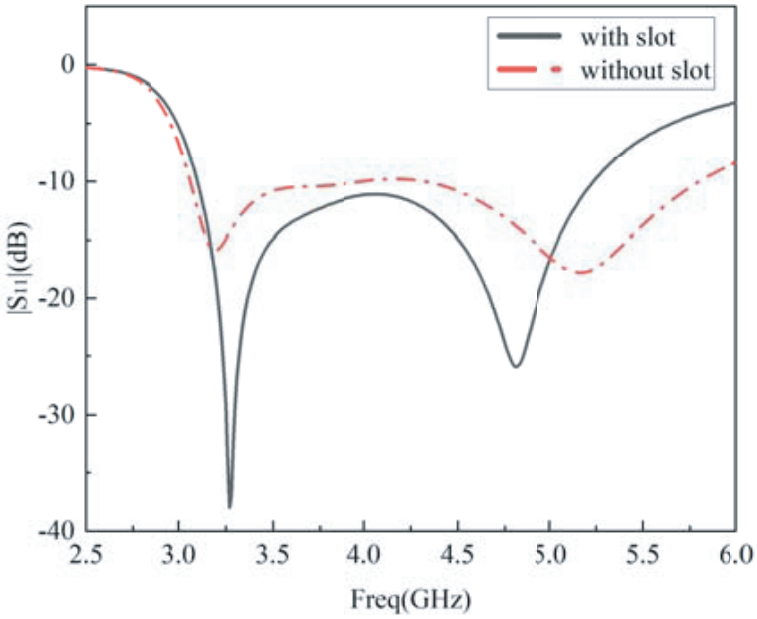

Figure 5. Return loss comparison between the ring patch with and without the fan slots.

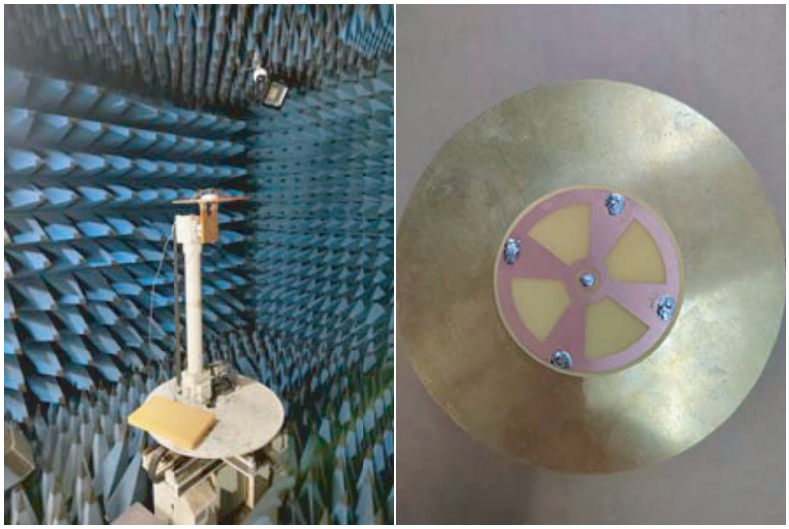

(a) (b)

Figure 6. The photograph of measurement and prototype.

3. MEASURED RESULTS

As shown in Fig. 6, a prototype of the proposed antenna is made and measured.

Figure 7 shows the compared antenna measurement and simulation of $|S_{11}|$ and VSWR, and their deviation may be manufacturing tolerance and caused by the error of measurement. The measured impedance bandwidth of 49.6% coverage ranges from 3.26 to 5.41 GHz, complete coverage of the 5G-N78 and N79 band. It can be seen that the simulation and measurement are basically consistent, and VSWR < 1.8 can be satisfied in the corresponding operating frequency band.

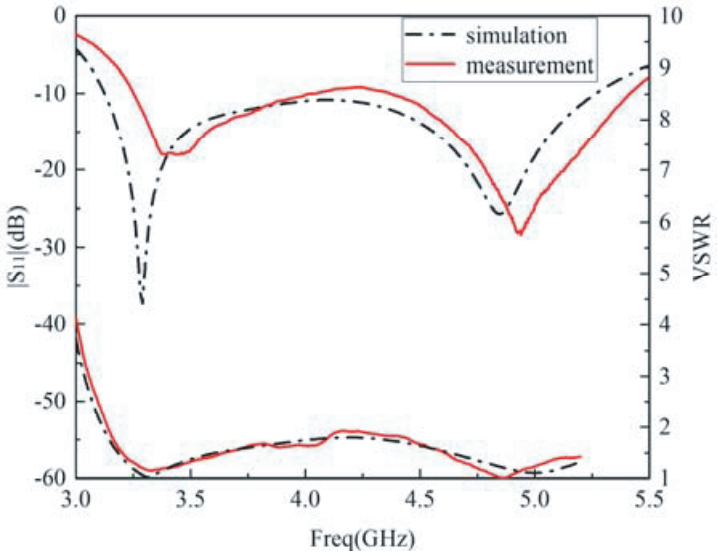

Figure 7. Simulated and measured S-parameter and VSWR of the proposed antenna.

Figure 8 depicts the simulated and measured gain curves. The peak gain of the proposed antenna varies from 2 to 7 dBi, and the maximum gain value can reach 6.8 dBi.

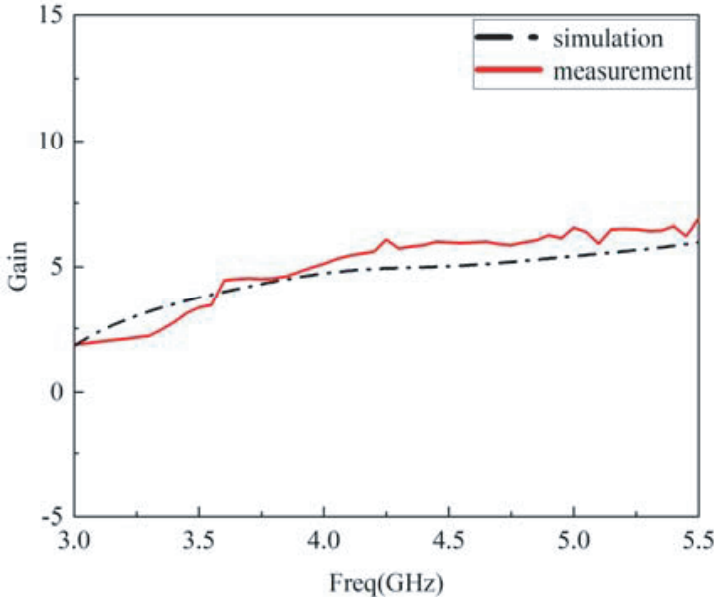

Figure 8. Simulated and measured peak gain of the proposed antenna.

Figure 9 shows the radiation pattern of the proposed antenna at 3.3, 3.5, 4.8, and 5.0 GHz, respectively. In terms of the overall shape, the antenna has a radiation pattern similar to that of a monopole, and the roundness of the horizontal plane is about 1 dB. Therefore, the proposed antenna has a relatively stable radiation pattern in the whole operating band. However, the measured cross-polarization level is obviously higher than the simulated results, which is caused by the insufficient accuracy of the feed and the limited SNR environment in the dark room.

In addition, several antenna parameters of the same type with similar monopole radiation characteristics are listed in Table 1. The specific comparison is mainly carried out from three aspects of profile height, bandwidth, and maximum gain. Compared to them, the antenna proposed in this paper has a lower profile and achieves a wider relative bandwidth and a higher peak gain.

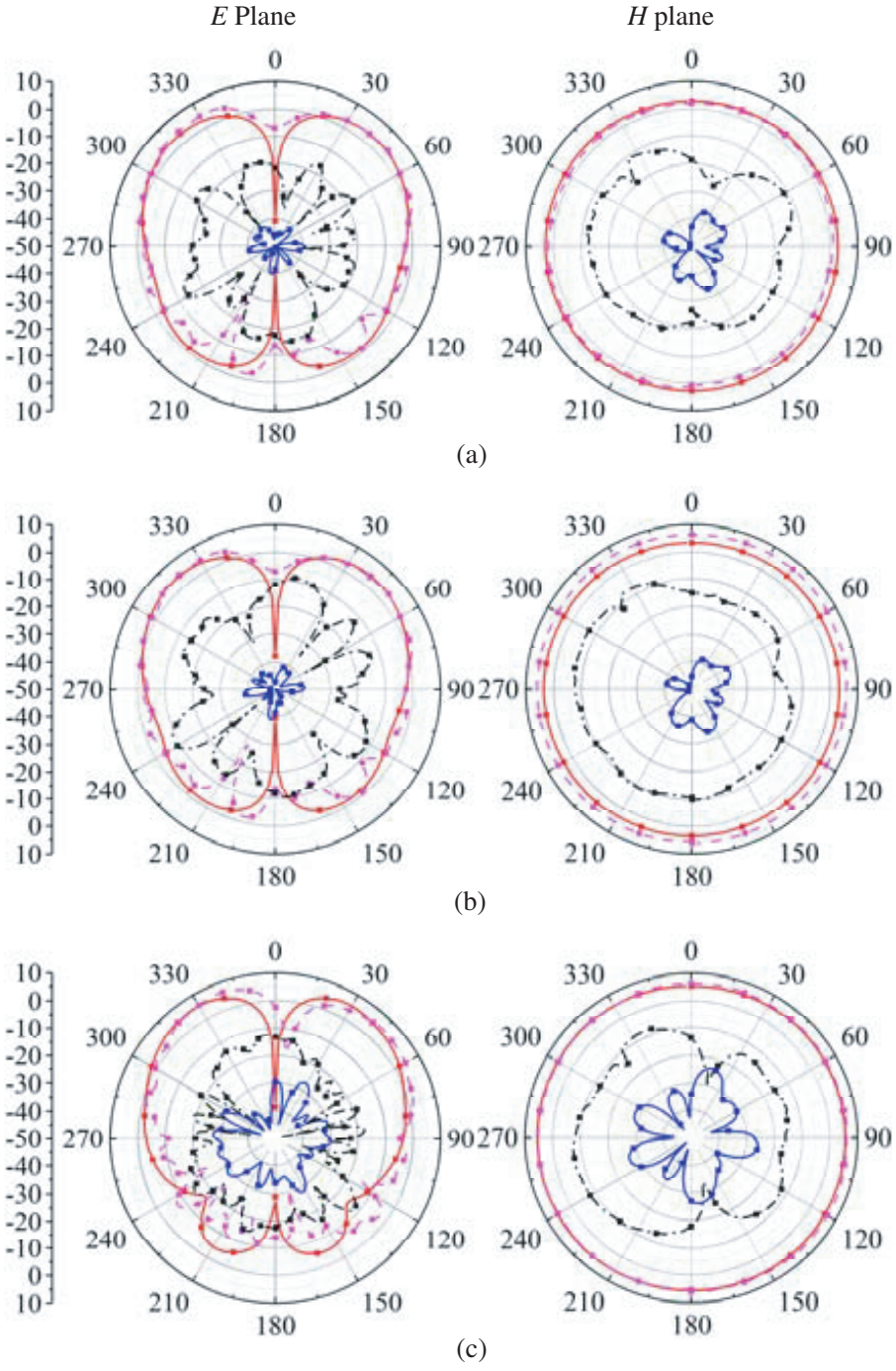

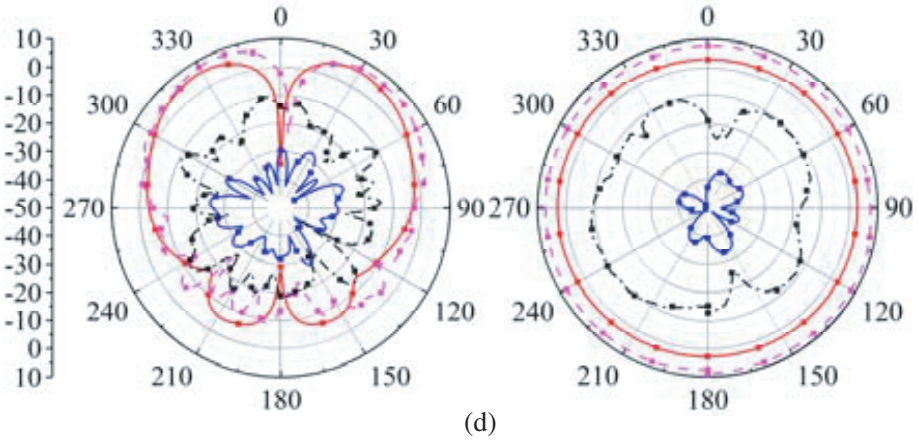

(d)

Figure 9. The simulation and measurement results of the proposed antenna radiation pattern in E-Plane (xoz plane) and H-Plane (xoy plane) at (a) 3.3 GHz, (b) 3.5 GHz, (c) 4.8 GHz, (d) 5 GHz. The solid red line and the dotted purple line represent the simulated and measured co-pol component; The blue solid line and the black dotted line represent the simulated and measured cross-pol component.

Table 1. Performance comparison of the proposed antenna with other existing antennas.

Ref.	Max. gain (dBi)	H (λ min)	BW
[1]	< 5	0.06	48.5%
[5]	< 4	0.092	50%
[7]	5.58	0.05	7.1%
[8]	< 3	0.092	27.1%
[9]	< 6.5	0.13	30%
[13]	6	0.024	18%
[14]	6	0.029	24%
Proposed	6.8	0.054	51%

4. CONCLUSION

An antenna suitable for 5G indoor micro base station is proposed. The required radiation mode is excited by using probe feeding in the center of a circle patch radiator with an annular slot, which completely covers 5G-N78/77/79 bands. In the whole operating frequency band, the voltage standing wave ratio is less than 1.8, and the peak gain can reach 2–7 dBi. The antenna has low processing cost and low profile, which can be used as a candidate for 5G indoor base station application.

REFERENCES

1. Wen, S. and Y. Dong, "A low-profile vertically polarized antenna with conical radiation pattern for indoor micro base station application," *IEEE Antennas Wireless Propag. Lett.*, Vol. 20, No. 2, Feb. 2021.
2. Lee, K. F. and K. M. Luk, *Microstrip Patch Antennas*, Imperial College Press, London, U.K., 2011.
3. Zhou, L., Y. Jiao, Y. Qi, Z. Weng, and L. Lu, "Wideband ceiling-mount omnidirectional antenna for indoor distributed antenna systems," *IEEE Antennas Wireless Propag. Lett.*, Vol. 13, 836–839, 2014.

4. Delaveaud, C., P. Leveque, and B. Jecko, "New kind of microstrip antenna: The monopolar wire-patch antenna," *Electron. Lett.*, Vol. 30, No. 1, 1–2, 1994.
5. Zhang, Z. Y., G. Fu, S. X. Gong, S. L. Zuo, and Q. Y. Lu, "Sleeve monopole antenna for DVB-H applications," *Election. Lett.*, Vol. 46, No. 13, 879–880, Jun. 2010.
6. Zuo, S. L., Y. Z. Yin, Z. Y. Zhang, and K. Song, "Enhanced bandwidth of low-profile sleeve monopole antenna for indoor base station application," *Electron. Lett.*, Vol. 46, No. 24, 1587–1588, Nov. 2010.
7. Al-Bawri, S. S., et al., "Multilayer base station antenna at 3.5 GHz for Future 5G Indoor Systems," *2019 First International Conference of Intelligent Computing and Engineering (ICOICE)*, 2019.
8. Lau, K. L. and K. M. Luk, "A wide-band monopolar wire-patch antenna for indoor base station applications," *IEEE Antenna Wireless Propag. Lett.*, Vol. 4, 155–157, 2005.
9. Guo, Y. X., M. Y. W. Chia, Z. N. Chen, and K. M. Luk, "Wide-band L-probe fed circular patch antenna for conical-pattern radiation," *IEEE Trans. Antennas Propag.*, Vol. 52, No. 4, 1115–1116, Apr. 2004.
10. Batchelor, J. C., K. Voudouris, and R. J. Langley, "Dual mode and stacked concentric ring patch antenna array," *Electron. Lett.*, Vol. 29, No. 15, 1319–1320, Jul. 1993.
11. Economou, L. and R. J. Langley, "Patch antenna equivalent to simple monopole," *Electron. Lett.*, Vol. 33, No. 9, 727–728, Apr. 1997.
12. González-Posadas, V., D. Segovia-Vargas, E. Rajo-Iglesias, J. L. Vázquez-Roy, and C. Martín-Pascual, "Approximate analysis of short circuited ring patch antenna working at TM_{01} mode," *IEEE Trans. Antennas Propag.*, Vol. 54, No. 6, 1875–1879, Jun. 2006.
13. Liu, J., Q. Xue, H. Wong, H. Lai, and Y. Long, "Design and analysis of a low-profile and broadband microstrip monopolar patch antenna," *IEEE Trans. Antennas Propag.*, Vol. 61, No. 1, 11–18, Jan. 2013.
14. Liu, J., S. Zheng, Y. Li, and Y. Long, "Broadband monopolar microstrip patch antenna with shorting vias and coupled ring," *IEEE Antennas Wireless Propag. Lett.*, Vol. 13, 39–42, 2014.
15. Wolff, I. and N. Knoppik, "Rectangular and circular microstrip disk capacitors and resonators," *IEEE Transactions on Microwave Theory and Techniques*, Vol. 22, No. 10, 857–864, Oct. 1974.